Section 5.0 : Horn Physics

Before discussing the design of a horn loaded loudspeaker system, it is really important to understand the physics that make a horn work. In the previous sections, all of the required relationships were derived and now they can be pulled together to understand and explain what really makes the horn geometry a highly efficient sound transmission device. Pulling equations and figures from Sections 2.0, 3.0, and 4.0 will hopefully produce a logical explanation of basic exponential horn physics.

Figure 5.1 shows the minimum geometry required to define an exponential horn. The area at the throat S_0, the area at the mouth S_L, and the length L are used to calculate the flare constant m of the exponential horn.

Figure 5.1 : Exponential Horn Geometry Definition

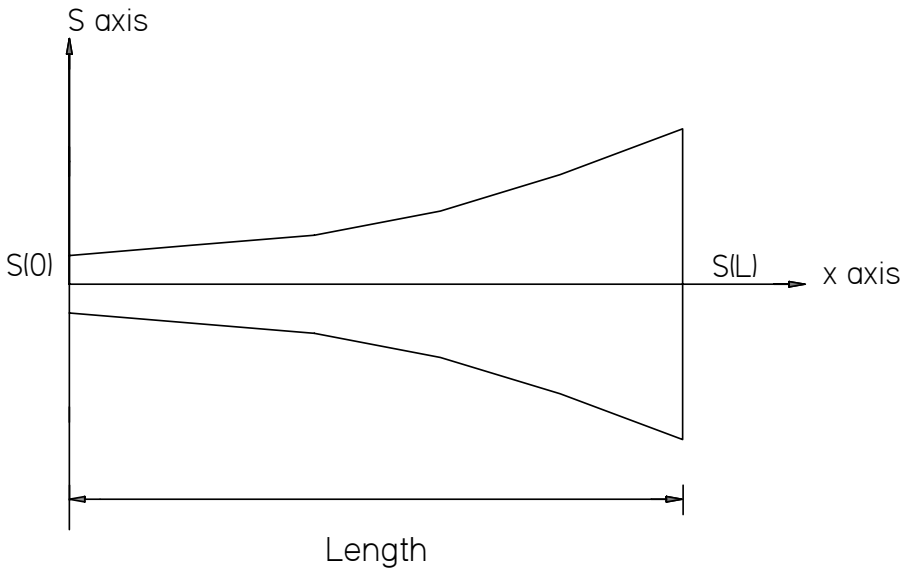

The exponential horn geometry is described by the following expression.

$$S(x) = S_0 \, \mathbf{e}^{(m\,x)}$$

At x = 0 and x = L

$$S(0) = S_0$$

$$S(L) = S_0 \, \mathbf{e}^{(m\,L)}$$

$$S(L) = S_L$$

Solving for the flare constant m

Equation (5.1)

$$m = \frac{\ln\left(\frac{S_L}{S_0}\right)}{L}$$

This is the first important relationship derived that will be used later in this section.

The next important relationship comes from the solution of the wave equation. Restating Equation (2.2), the one dimensional damped wave equation, and setting the damping term λ to zero leaves the classic exponential horn wave equation that can be found in most acoustics texts.

$$c^2\left(\left(\frac{\partial}{\partial x}\left(\frac{\partial}{\partial x}\xi(x,t)\right)\right)+m\left(\frac{\partial}{\partial x}\xi(x,t)\right)\right)=\frac{\partial}{\partial t}\left(\frac{\partial}{\partial t}\xi(x,t)\right)$$

Assuming a solution of the form

$$\xi(x,t) = \Xi(x)\,\mathbf{e}^{(I\,\omega\,t)}$$

separates the time and displacement variables in the solution leaving a second order differential equation containing only the displacement variable as shown below.

$$\left(\frac{\partial^2}{\partial x^2}\Xi(x)\right)+m\left(\frac{\partial}{\partial x}\Xi(x)\right)+\frac{\Xi(x)\,\omega^2}{c^2}=0$$

Assuming a displacement solution of the form

$$\Xi(x) = \mathbf{e}^{(-I\,\gamma\,x)}$$

generates the characteristic equation

$$-\gamma^2 - I\,\gamma\,m + \frac{\omega^2}{c^2} = 0$$

where

$$\gamma = \frac{-I\,m\,c + \sqrt{4\,\omega^2 - m^2\,c^2}}{2\,c}, \frac{-I\,m\,c - \sqrt{4\,\omega^2 - m^2\,c^2}}{2\,c}$$

$$\gamma = -I\,\alpha + \beta, -I\,\alpha - \beta$$

Substituting this expression into the assumed solution for the displacement, and then back into the originally assumed time dependent solution, results in the following general solution

$$\xi(x, t) = (C_1\,\mathbf{e}^{((-\alpha - I\,\beta)\,x)} + C_2\,\mathbf{e}^{((-\alpha + I\,\beta)\,x)})\,\mathbf{e}^{(I\,\omega\,t)}$$

where

$$\alpha = \frac{m}{2}$$

$$\beta = \frac{\sqrt{4\,\omega^2 - m^2\,c^2}}{2\,c}$$

The first term, α, is an attenuation term arising from the expanding geometry. The roll of the second term, β, depends on the value of the frequency under the radical symbol. If $(4\omega^2\text{-}m^2c^2) < 0$ then β is imaginary and results in an additional exponential attenuation term. If $(4\omega^2\text{-}m^2c^2) > 0$ then β is real and wave motion exists in the horn. The frequency at which the transition, from attenuation to wave motion, occurs when $(4\omega^2\text{-}m^2c^2) = 0$. This transition frequency can be derived as follows

$$4\,\omega^2 - m^2\,c^2 = 0$$

leading to Equation (5.2) for the lower cut-off frequency f_c of an exponential horn.

Equation (5.2)

$$f_c = \frac{m\,c}{4\,\pi}$$

From Equation (5.2), the lower cut-off frequency of an exponential horn can be calculated given a flare constant m. But more likely the case when designing a horn the required flare constant m will be calculated after assuming a lower cut-off frequency f_c.

Referring back to Section 3.0, the point at which a circular or square horn mouth starts to efficiently transfer energy into the environment occurs when $(2\ k\ a_L) = 2$. Combining this result with Equation (5.2), an expression for the minimum mouth area of a circular or square cross-section horn can be derived. This expression is independent of horn's flare geometry.

Equation (5.3)

$$S_L = \frac{\left(\frac{c}{2 f_c}\right)^2}{\pi}$$

If a value for the lower cut-off frequency f_c is defined, then Equations (5.2) and (5.3) can be used to determine the flare constant m and the circular or square mouth cross-sectional area S_L. Then if either the horn's length L or throat area S_0 is assigned, consistent exponential horn geometry is completely defined by applying Equation (5.1).

Design of an Exponential Horn Tuned to 100 Hz :

Assuming that the desired lower cut-off frequency f_c of an exponential horn is 100 Hz, an infinite number of horn geometries can be specified. All of these geometries will have a common mouth area and flare constant as defined by Equations (5.2) and (5.3).

$$m = (4\ \pi\ f_c) / c$$

$$m = (4\ \pi\ 100\ \text{Hz}) / (344\ \text{m/sec})$$

$$m = 3.653\ \text{m}^{-1}$$

$$S_L = (c / (2\ f_c))^2 / \pi$$

$$S_L = ((344\ \text{m/sec}) / (2 \times 100\ \text{Hz}))^2 / \pi$$

$$S_L = 0.942\ \text{m}^2$$

The last two unknown properties of the exponential horn are the throat area S_0 and the length L. If one variable is assumed, the other one can be calculated using Equation (5.1). Table 5.1 lists four different consistent exponential horn geometries derived assuming different values for the throat area S_0.

When the set of Equations (5.1), (5.2), and (5.3) are used to calculate the throat area, flare constant, mouth area, and length of an exponential horn assuming a single tuning frequency f_c, then I define this as a consistent horn geometry. All of the dimensions are calculated based on the same lower cut-off frequency f_c. If one or some of the dimensions are calculated or assigned in an inconsistent manner, then I consider this a compromised horn geometry.

Table 5.1 : Four Consistent Exponential Horn Geometries Tuned to 100 Hz

Horn	S_L	S_L / S_0	S_0	L	Figure
A	0.942	5	0.188	0.441	5.2
B	0.942	10	0.094	0.630	5.3
C	0.942	20	0.047	0.820	5.4
D	0.942	40	0.024	1.010	5.5
Units	m^2	---	m^2	m	---

Figures 5.2, 5.3, 5.4, and 5.5 show the acoustic impedance at the throat, and the ratio of the volume velocities, for the horn geometries defined in Table 5.1. Several interesting observations can be made after studying these four plots.

Comparing the acoustic impedance curves, the top two plots in each figure, shows that above the lower cut-off frequency the impedance magnitude approaches a constant ρ x c / S_0. In the phase plot, the phase approaches zero above the lower cut-off frequency. The acoustic impedance at the throat of an exponential horn becomes predominantly resistive above the lower cut-off frequency and has an easily predicted magnitude and phase. As the horn's throat becomes smaller, the acoustic resistance rises which in turn increases the horn's efficiency. This acoustic resistance is seen by one side of the driver's moving cone depending on whether the horn design being considered is a front loaded or a back loaded horn.

The ratio of the volume velocities, the bottom two plots in each figure, shows that above the lower cut-off frequency of an exponential horn the volume velocity at the mouth is greater then the applied volume velocity at the throat. As the horn length increases, the throat area decreases, and the ratio of the volume velocities grows. The sound pressure level produced by the horn mouth is a function of the mouth's volume velocity. Therefore, as the exponential horn's length increases, for a given mouth area, the SPL output of the horn also increases.

Figure 5.2 : Acoustic Impedance and Volume Velocity Ratio for Horn “A” in Table 5.1

Acoustic Impedance at the Throat of the Horn

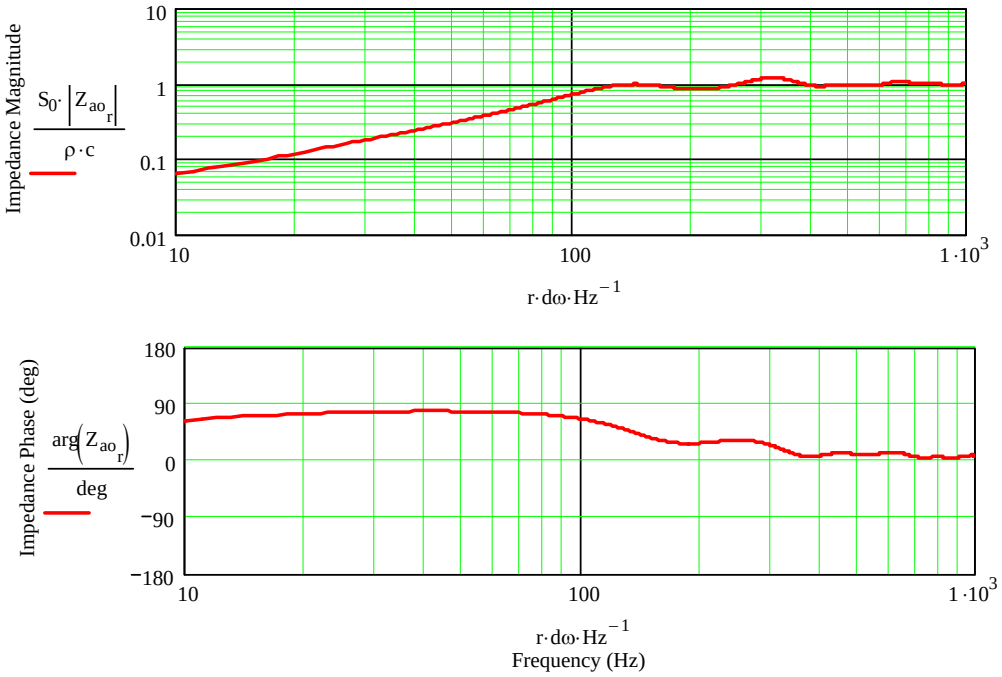

E = (Volume Velocity at the Mouth of the Horn) / (Volume Velocity at the Throat of the Horn)

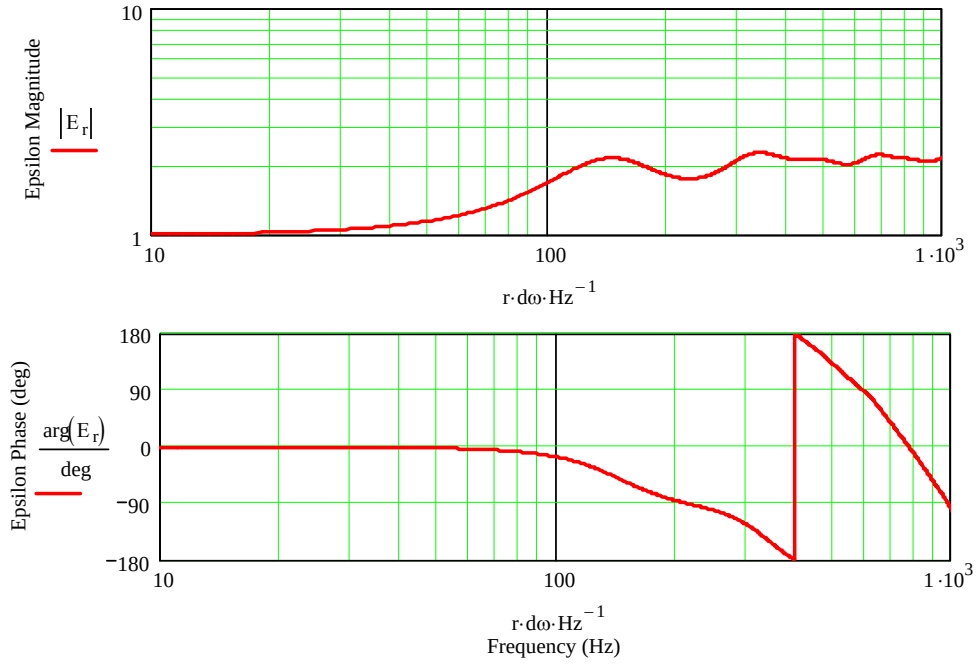

Figure 5.3 : Acoustic Impedance and Volume Velocity Ratio for Horn “B” in Table 5.1

Acoustic Impedance at the Throat of the Horn

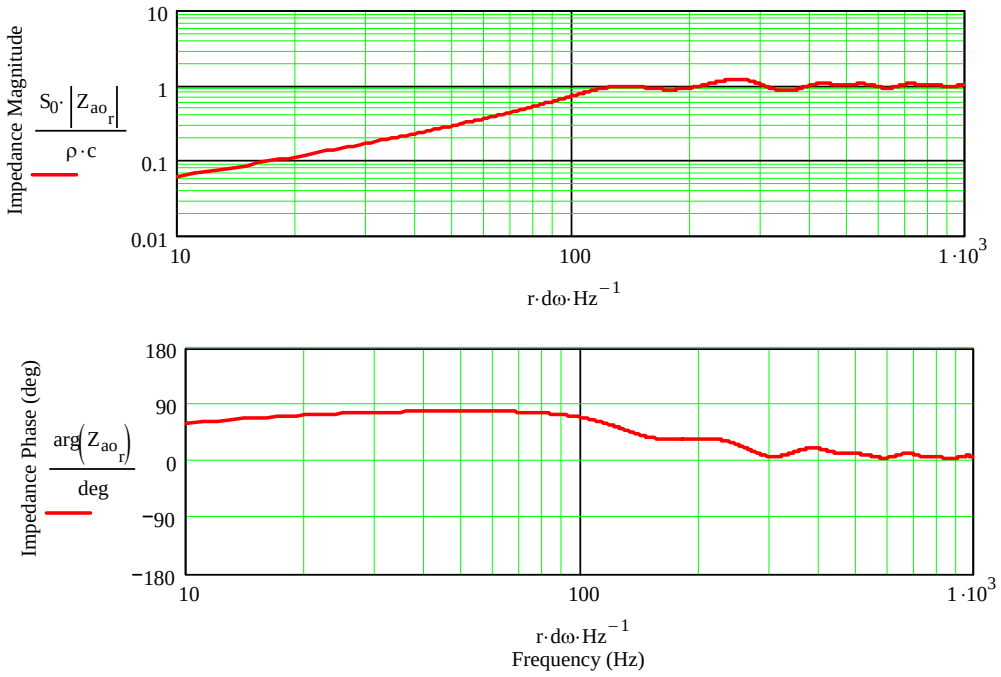

E = (Volume Velocity at the Mouth of the Horn) / (Volume Velocity at the Throat of the Horn)

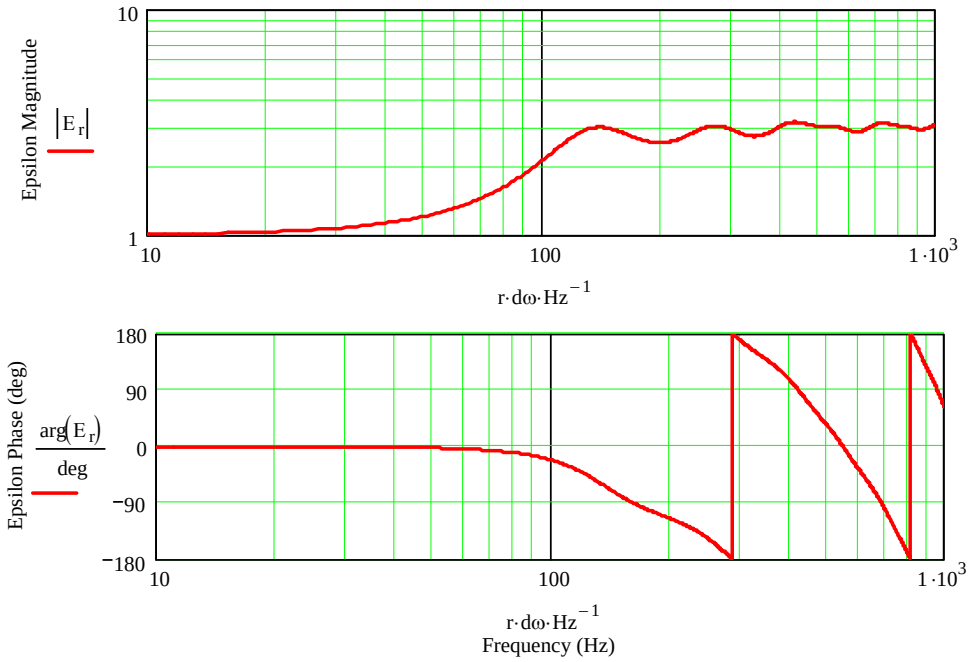

Figure 5.4 : Acoustic Impedance and Volume Velocity Ratio for Horn “C” in Table 5.1

Acoustic Impedance at the Throat of the Horn

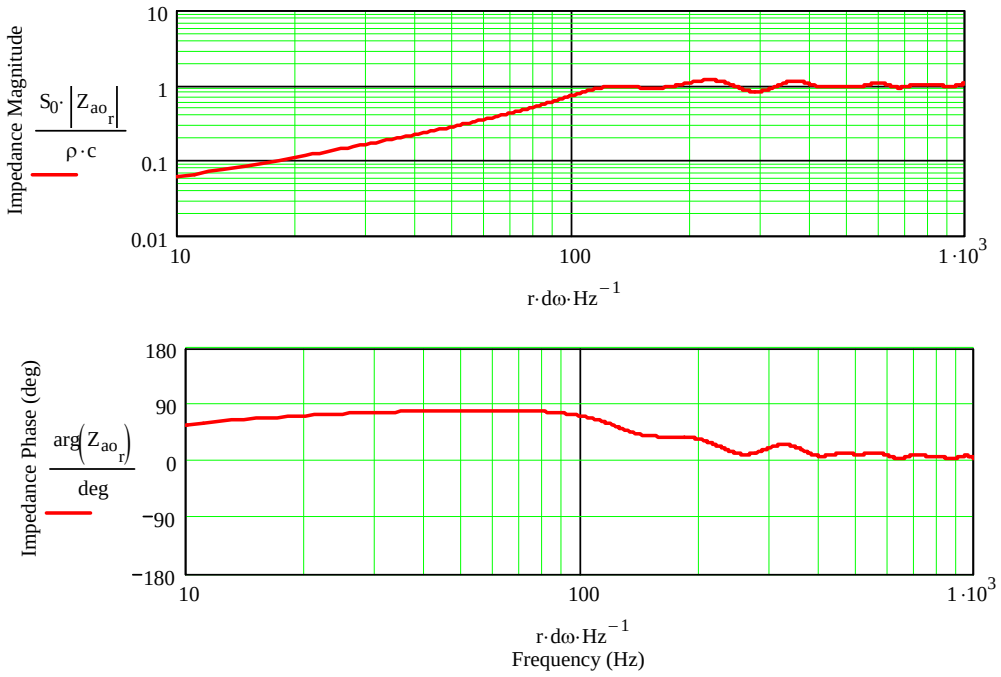

E = (Volume Velocity at the Mouth of the Horn) / (Volume Velocity at the Throat of the Horn)

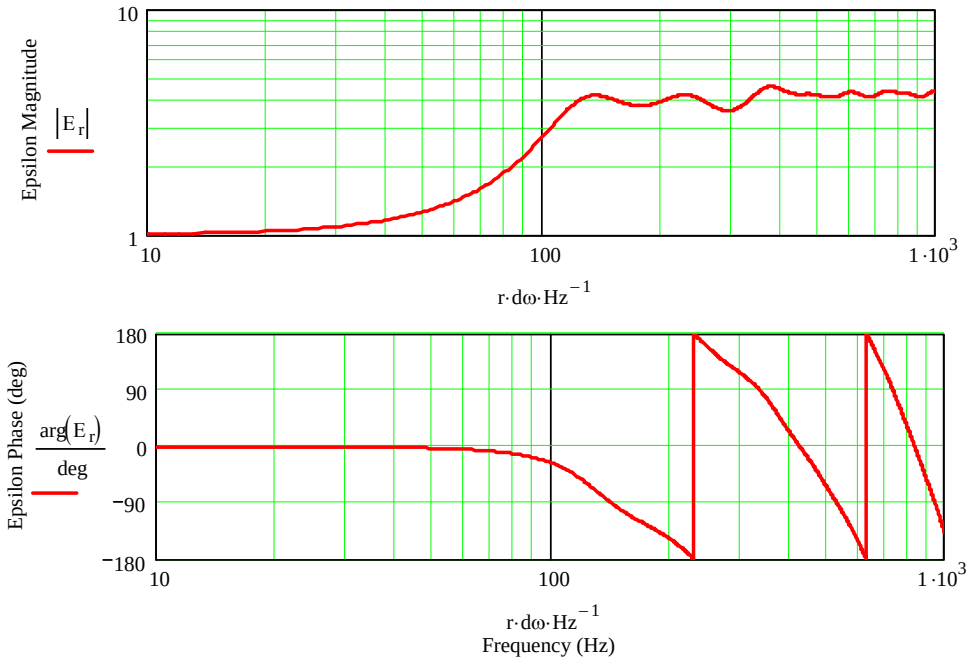

Figure 5.5 : Acoustic Impedance and Volume Velocity Ratio for Horn “D” in Table 5.1

Acoustic Impedance at the Throat of the Horn

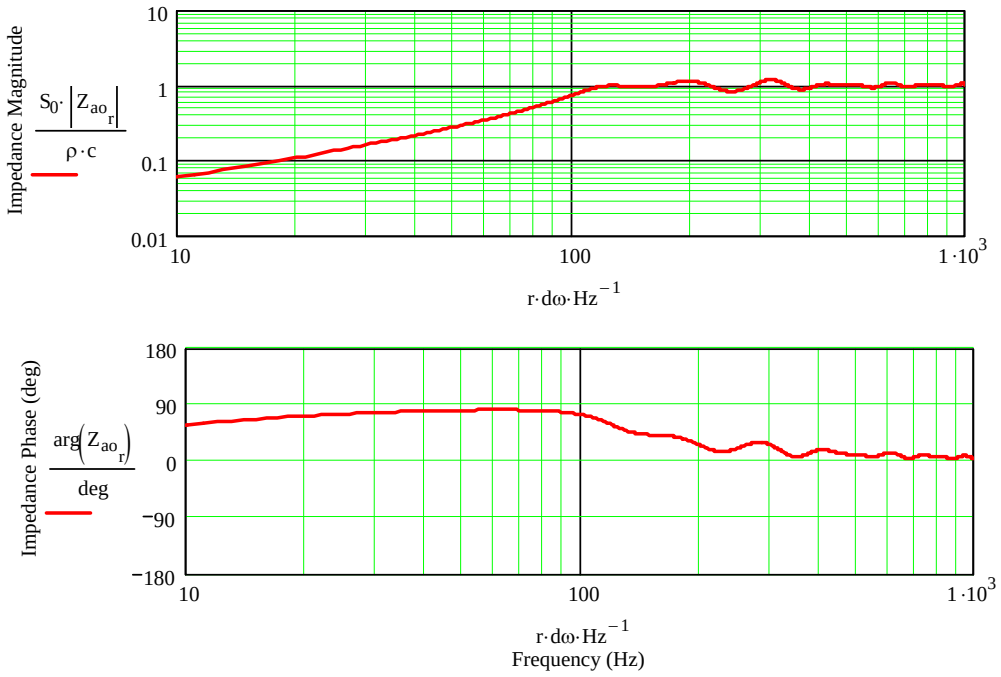

E = (Volume Velocity at the Mouth of the Horn) / (Volume Velocity at the Throat of the Horn)

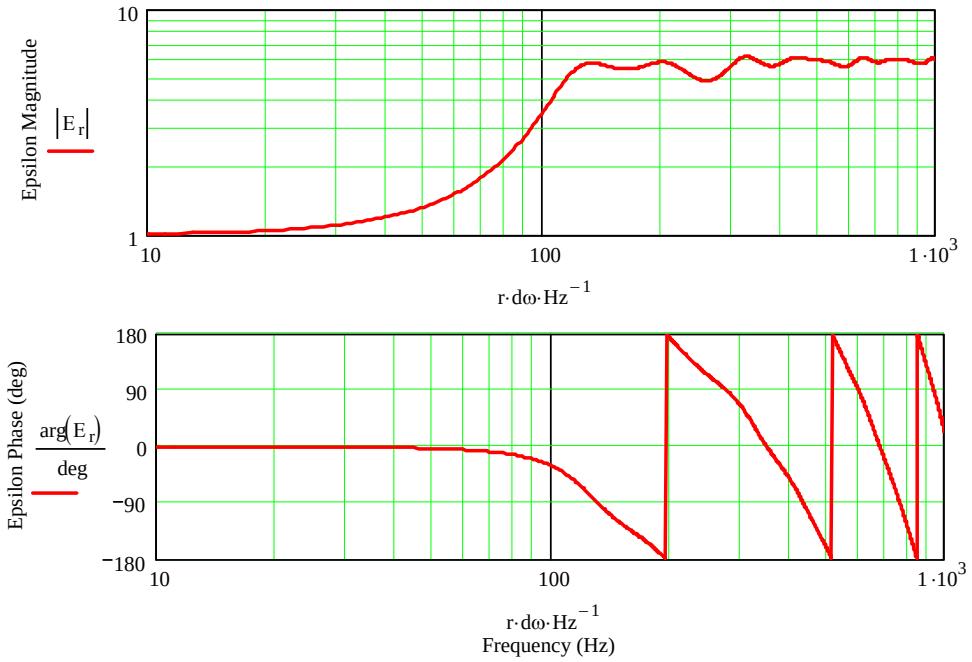

Design of a Coupling Volume :

Combining the resistive nature of the throat acoustic impedance, above the lower cut-off frequency f_c, with a small coupling volume produces a higher cut-off frequency f_h. Figure 5.6 shows the acoustic equivalent circuit of an exponential horn with a small coupling volume, between the driver and the throat, at frequencies well above the lower cut-off frequency f_c.

Figure 5.6 : Equivalent Acoustic Circuit of an Exponential Horn
with a Coupling Volume Between the Driver and the Throat

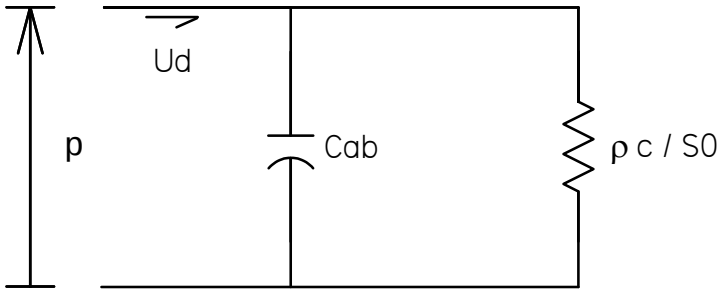

The equivalent circuit in Figure 5.6 is a first order acoustic cross-over network, similar to a first order low pass electrical crossover filter. The throat impedance and the compliance of the small coupling volume are given by the following expressions.

$$Z_{throat} = \frac{\rho\, c}{S_0}$$

$$C_{ab} = \frac{V}{\rho\, c^2}$$

At the higher cut-off frequency f_h, by definition the impedance magnitudes of the throat and the coupling volume must be equal. This results in the driver's volume velocity U_d being split equally between the coupling volume and the throat impedance.

$$\frac{1}{2\,\pi\, f_h\, C_{ab}} = \frac{\rho\, c}{S_0}$$

Substituting and solving for the coupling volume produces the required expression.

Equation (5.4)

$$V = \frac{c\, S_0}{2\,\pi\, f_h}$$

To add a coupling volume to Horn “C”, from Table 5.1 and plotted in Figure 5.4, the following calculation is performed assuming that a higher cut-off frequency of 500 Hz is desired.

$$V = (344 \text{ m/sec} \times 0.047 \text{ m}^2) / (2 \pi 500 \text{ Hz}) \times (1000 \text{ liters} / \text{m}^3) = 5.146 \text{ liters}$$

Placing this coupling volume in series with the geometry of Horn “C”, and rerunning the MathCad calculation, yields the results plotted in Figure 5.7. Figure 5.7 exhibits a high frequency roll-off of both the throat acoustic impedance and the volume velocity ratio as anticipated.

Figure 5.7 : Acoustic Impedance and Volume Velocity Ratio for Horn “C” in Table 5.1 with a 5 liter Coupling Volume

Acoustic Impedance at the Throat of the Horn

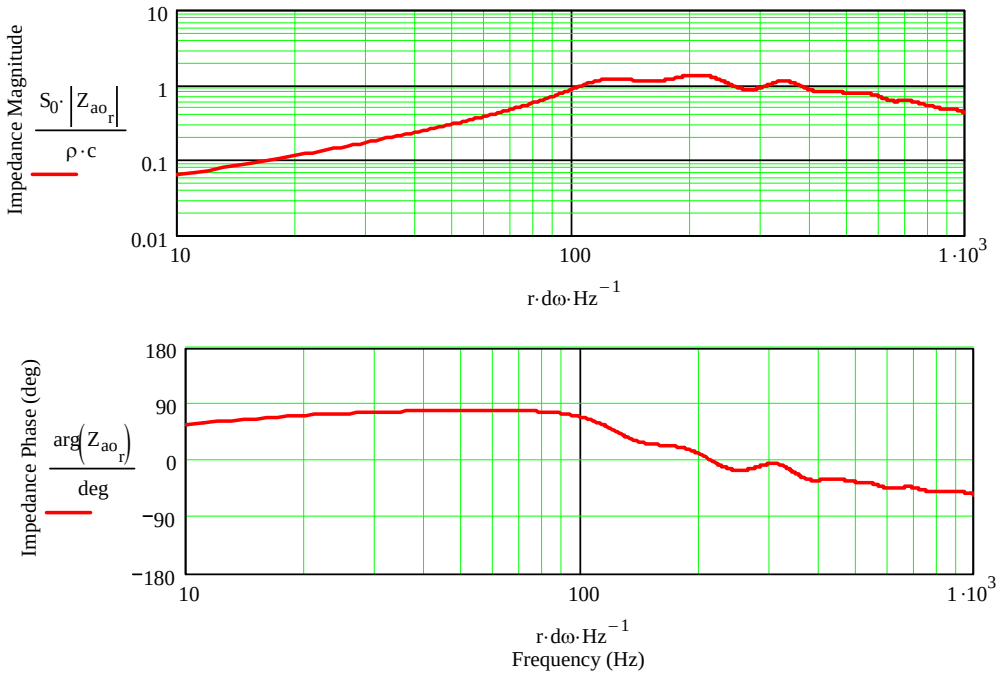

E = (Volume Velocity at the Mouth of the Horn) / (Volume Velocity at the Throat of the Horn)

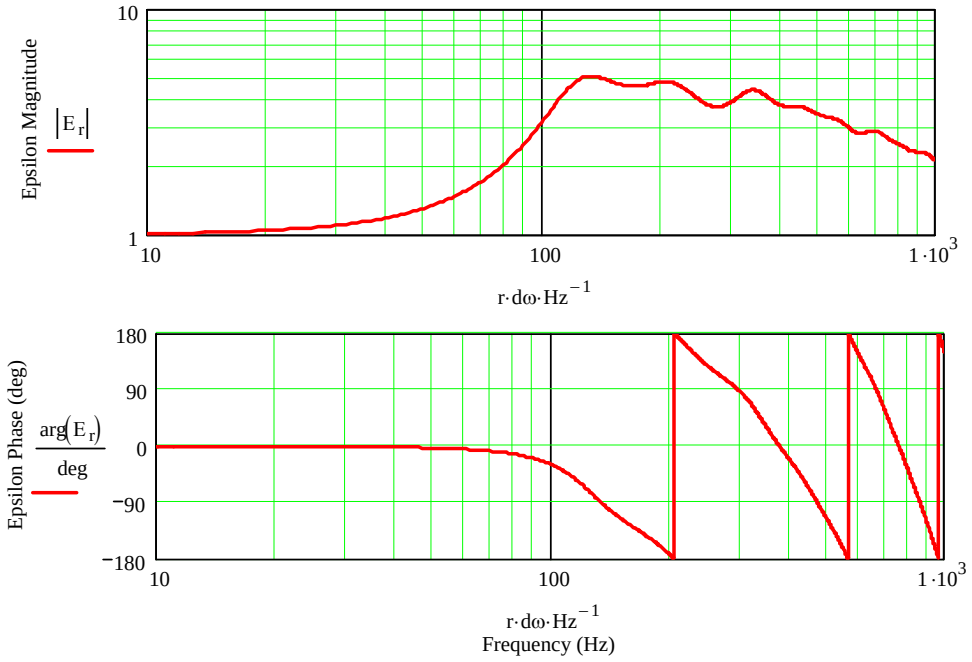

How an Exponential Horn Works :

To understand how an exponential horn works, let's start with a straight transmission line and plot the acoustic impedance at the driver end and the ratio of the volume velocities as was done in the preceding section. By incrementally increasing the cross-sectional area of the transmission line's open end, changes in the plotted results demonstrate the physics involved in the workings of an exponential horn. Table 5.2 summarizes the geometries used for this study. In Table 5.2, the lower cut-off frequency f_c is calculated based on the open end (the horn's mouth) cross-sectional area.

Table 5.2 : Exponential Horn Geometries Based on Horn C in Table 5.1

Horn	S_0	S_L / S_0	S_L	L	f_c	Figure
a	0.047	1	0.047	0.820	447.2	5.8
b	0.047	2	0.094	0.820	316.2	5.9
c	0.047	3	0.141	0.820	258.2	5.10
d	0.047	4	0.188	0.820	223.6	5.11
e	0.047	5	0.235	0.820	200.0	5.12
f	0.047	10	0.471	0.820	141.4	5.13
g	0.047	15	0.706	0.820	115.4	5.14
h	0.047	20	0.942	0.820	100.0	5.15
Units	m^2	---	m^2	m	Hz	---

Figure 5.8 shows the results for the straight transmission line. The fundamental resonance in the impedance plot occurs at 92 Hz which matches within 5% the calculated quarter wavelength prediction for a straight transmission line. In the quarter wavelength calculation the physical length is increased to include an end correction term.

$$f_0 = c / (4 \times L_{effective})$$
$$f_0 = (344 \text{ m/sec}) / (4 \times (0.820 \text{ m} + 0.6 \times ((0.047 \text{ m}^2) / \pi)^{1/2})) = 96 \text{ Hz}$$

The subsequent resonant peaks are at 3, 5, 7, …. multiples of the fundamental 1/4 wavelength frequency. The height and sharpness of the peaks, in the impedance and the volume velocity ratio plots, decrease as frequency increases due to the rising resistive (real) component of the open end's acoustic impedance. The typical acoustic impedance of the circular open end of a quarter wavelength resonator is plotted in Figure 5.16.

Figure 5.9 shows the plots for an expanding transmission line geometry that has twice the open end area as the original straight transmission line plotted in Figure 5.8. Notice that the fundamental resonance has increased from 92 Hz to 103 Hz. Also, all of the peaks and nulls are a little less pronounced and broader. This is an inconsistent or compromised horn geometry as defined at the top of page 3.

Figures 5.10, 5.11, and 5.12 continue to increase the open end area. As the heights of the peaks in the acoustic impedance and volume velocity ratio plots decrease and broaden, the valleys between successive peaks start to fill in and the lower bound of the plotted data rises. In each sequential plot, the acoustic damping provided by the open end increases and extends lower in the frequency range. The lower cut-off frequency f_c is dropping in frequency as the open end's cross-sectional area increases.

By Figure 5.13 the acoustic impedance is settling in and oscillating only slightly about (ρ x c) / S_0 while the ratio of volume velocities is approaching a constant value of three for frequencies above 300 Hz. The phase angles also show none of the large 180 degree phase swings typically associated with acoustic resonances. Figures 5.13 and 5.14 both appear to duplicate the horn responses seen in the earlier plots and again in Figure 5.15. The last horn geometry shown in Table 5.2 and Figure 5.15 is the consistent horn geometry since all of the parameters are tuned to a lower cut-off frequency f_c of 100 Hz, all of the other rows in Table 5.2 are compromised horn geometries.

To summarize the results shown in Figures 5.8 through 5.15, the geometric transition from straight unstuffed transmission line to consistent exponential horn geometry was studied by increasing the open end cross sectional area. The study held the length and the driven end cross sectional area constant while maintaining exponentially flared geometries. The geometries that lie between the transmission line and the final consistent exponential horn are all compromised exponential horn designs. The first observation made was that the fundamental quarter wavelength resonant frequency of the transmission line rose as the geometry expanded along the length. This is consistent with expanding TL design results described elsewhere on this site.

At the same time, increasing the open end's area increased the acoustic damping boundary condition. This results in the attenuation and broadening of the resonant peaks, and filling in of the deep nulls that exist between these peaks, typically associated with the higher harmonics of a transmission line's fundamental quarter wavelength resonance. As the expanding transmission line's open end area continued to increase, this effect started to become more evident at lower harmonics and eventually even at the fundamental resonant frequency. The damped resonant peaks spread and merge, filling in the valleys between them, producing relatively constant acoustic impedance above the lower cut-off frequency f_c. As transmission line geometry transitions to a consistent exponential horn there is no longer evidence of discrete standing waves, at distinct frequencies, producing a series of sharp peaks and nulls in the plotted responses.

A properly sized and designed exponential horn, a consistent design, is a non-resonant or in other words highly damped acoustic enclosure. Without the full damping supplied by the mouth, compromised exponential horns exhibit quarter wavelength standing waves similar to a transmission line enclosure. This counters one prevailing myth about standing waves in horns; there are no half wavelength standing wave resonances associated with a horn. All longitudinal standing wave resonances, in transmission lines and compromised horn geometries, exhibit quarter wavelength pressure and velocity distributions.

To understand the increased efficiency attributed to horn loading a driver, the volume velocity ratio Ξ has been plotted in the bottom two plots of Figures 5.8 through 5.15. Volume velocity at the open end is important because it can be used directly to calculate the pressure and thus the SPL at some position out in the listening environment. In all of the plots the volume velocity ratio at 10 Hz is equal to unity, so what goes in one end comes out of the other. But as we move up above 100 Hz, the transmission line response is seen as a series of tall narrow peaks while the more horn

like response becomes an elevated value across all frequencies. The volume velocity ratio Ξ in Figures 5.8 exhibits discrete peaks the first exceeding a ratio of 5 while the remaining peaks are all below a ratio of 5. Comparing this to Figure 5.15, the volume velocity ratio above 100 Hz is consistently hovering between 4 and 5. The series of plots 5.9 to 5.14 track the changes that take place in the volume velocity ratio curve as the geometry transitions from transmission line to consistent exponential horn geometry.

Extending these observations about the volume velocity ratio curves, to the acoustic SPL output produced by transmission lines and consistent exponential horns, leads to the following understanding of why the horn speaker is so efficient. The damping provided by the real part of the acoustic impedance at the horn's mouth efficiently transfers sound energy into the listening room environment at all frequencies above the lower cut-off frequency f_c. Without this constant transfer of energy, a significant portion of the sound energy would be reflected back into the flared geometry producing standing waves at discrete frequencies related to the length and flare rate. These standing waves produce narrow bands of higher SPL in the listening room due to the peaking resonance of the volume velocity at the open end. The consistent horn's efficient transfer of sound energy into the room produces a more uniform higher SPL output across the frequency spectrum and removes the potential for peaky acoustic output due to axial standing waves associated with a transmission line or compromised horn designs.

Figure 5.8 : Acoustic Impedance and Volume Velocity Ratio for S_L / S_0 = 1 in Table 5.2

Acoustic Impedance at the Throat of the Horn

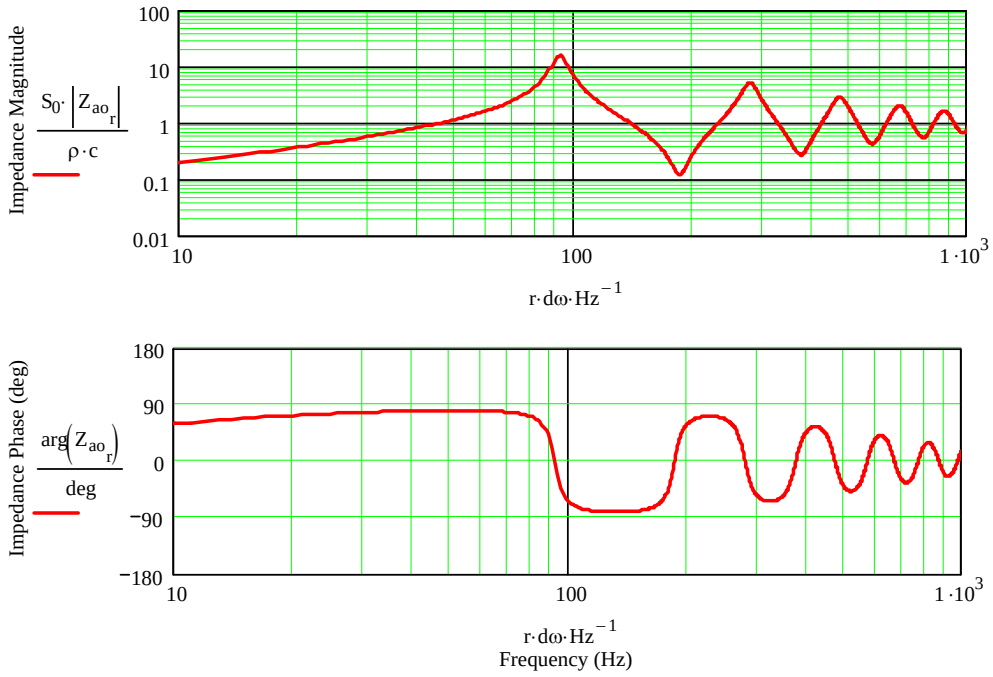

E = (Volume Velocity at the Mouth of the Horn) / (Volume Velocity at the Throat of the Horn)

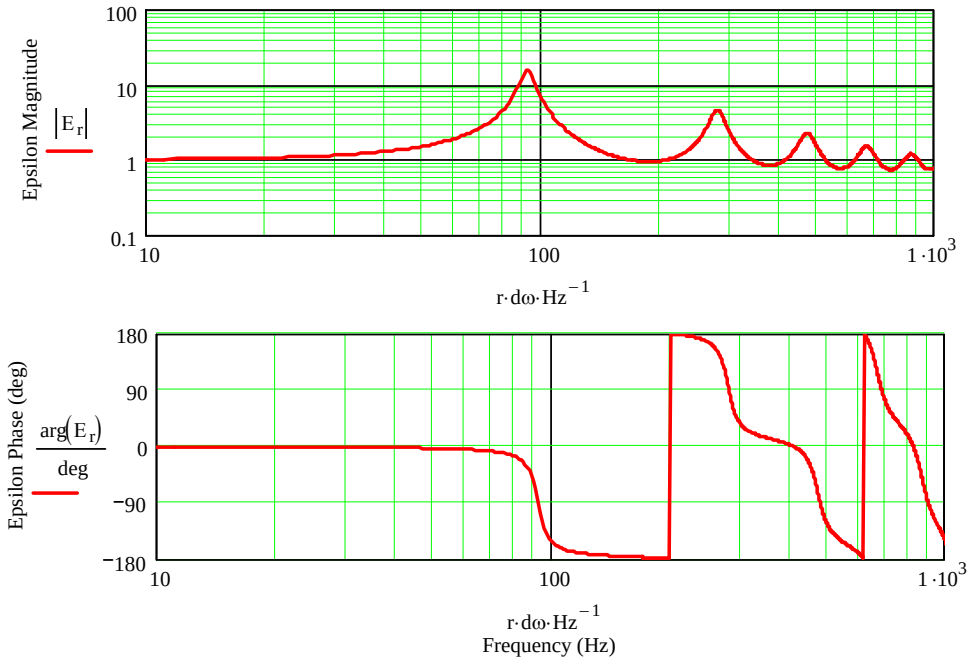

Figure 5.9 : Acoustic Impedance and Volume Velocity Ratio for S_L / S_0 = 2 in Table 5.2

Acoustic Impedance at the Throat of the Horn

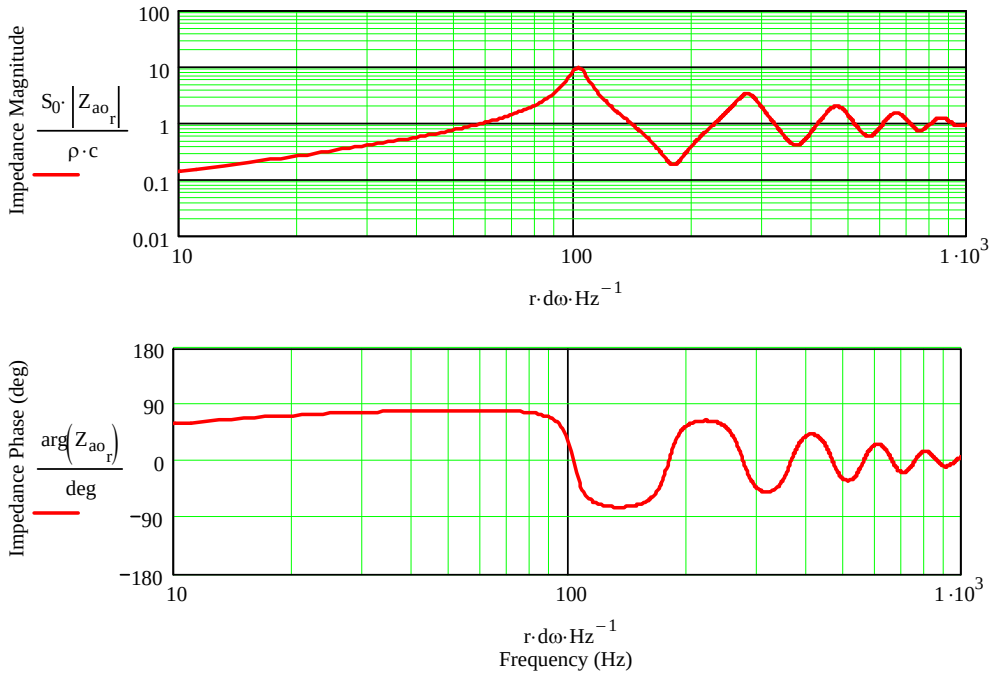

E = (Volume Velocity at the Mouth of the Horn) / (Volume Velocity at the Throat of the Horn)

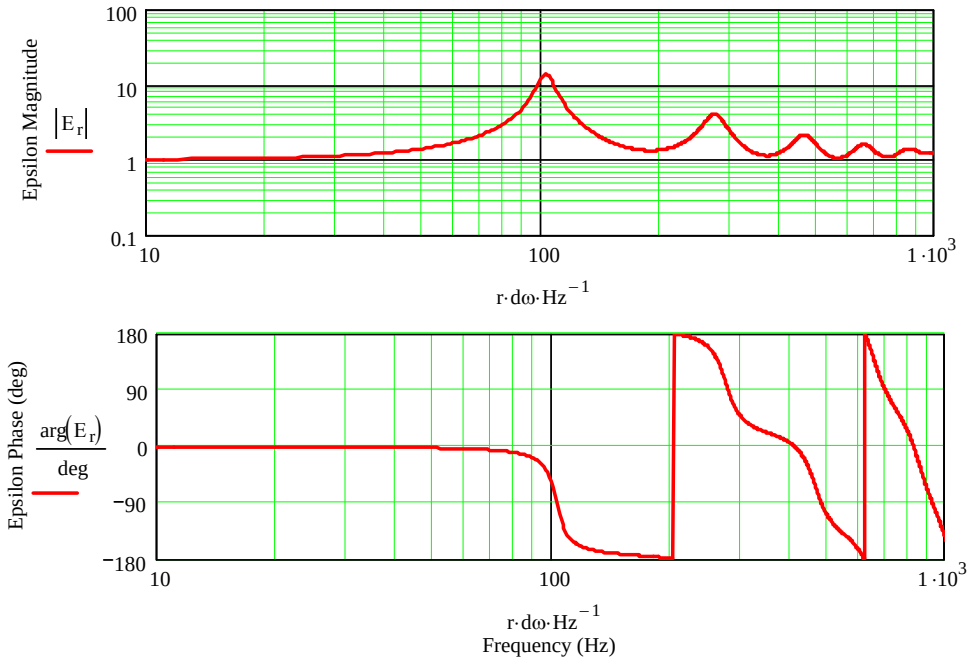

Figure 5.10 : Acoustic Impedance and Volume Velocity Ratio for S_L / S_0 = 3 in Table 5.2

Acoustic Impedance at the Throat of the Horn

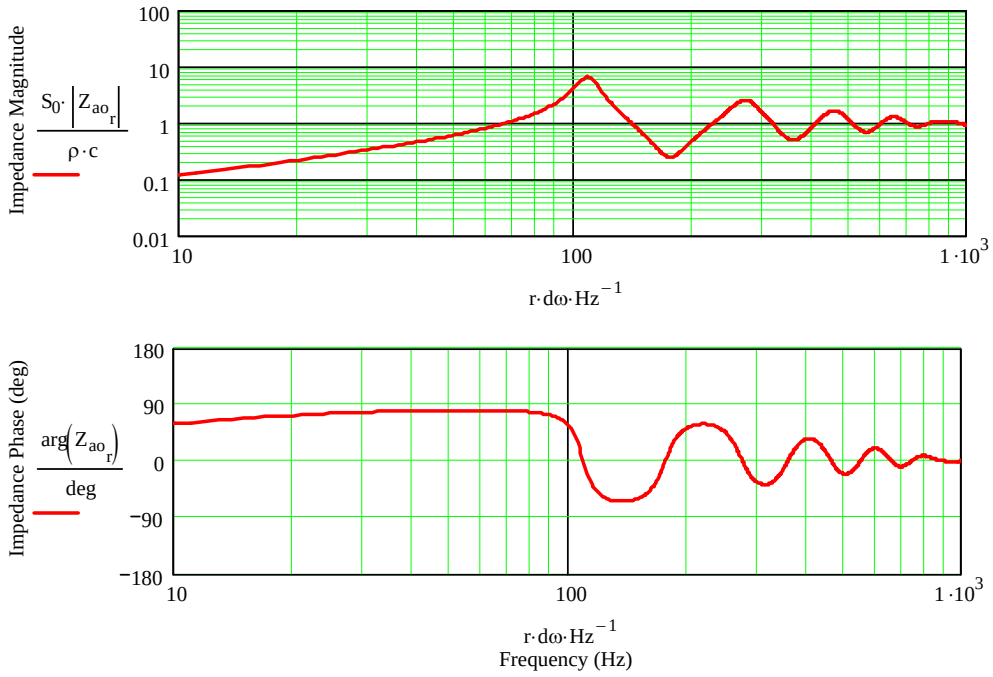

E = (Volume Velocity at the Mouth of the Horn) / (Volume Velocity at the Throat of the Horn)

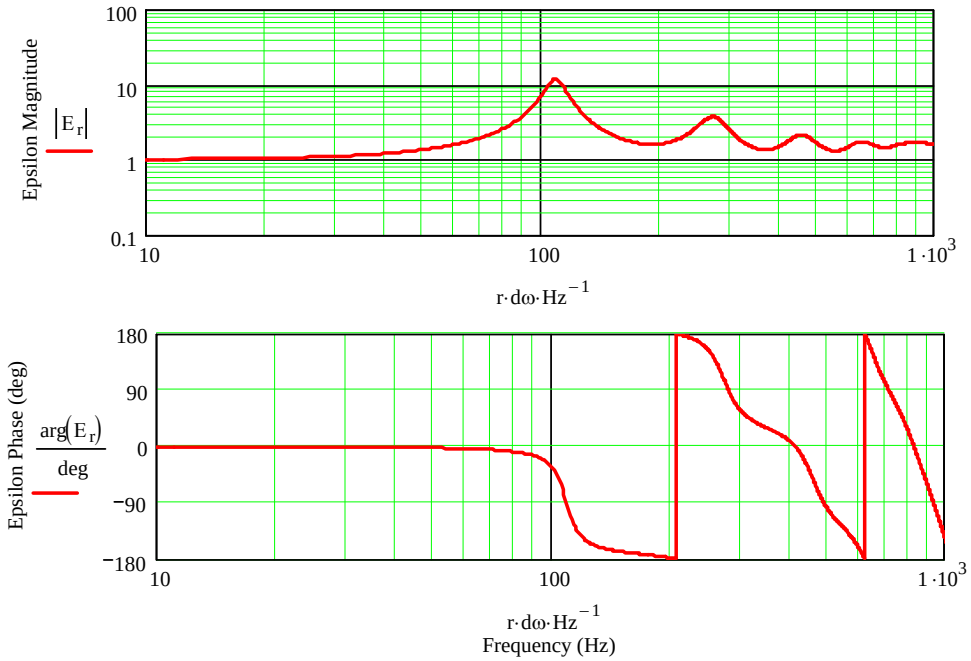

Figure 5.11 : Acoustic Impedance and Volume Velocity Ratio for S_L / S_0 = 4 in Table 5.2

Acoustic Impedance at the Throat of the Horn

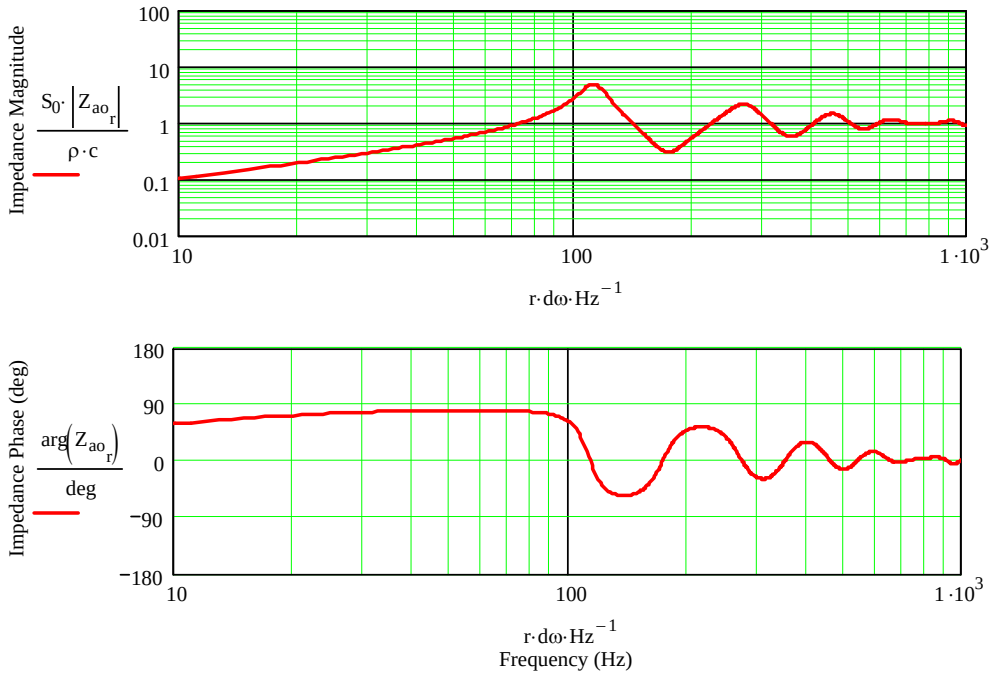

E = (Volume Velocity at the Mouth of the Horn) / (Volume Velocity at the Throat of the Horn)

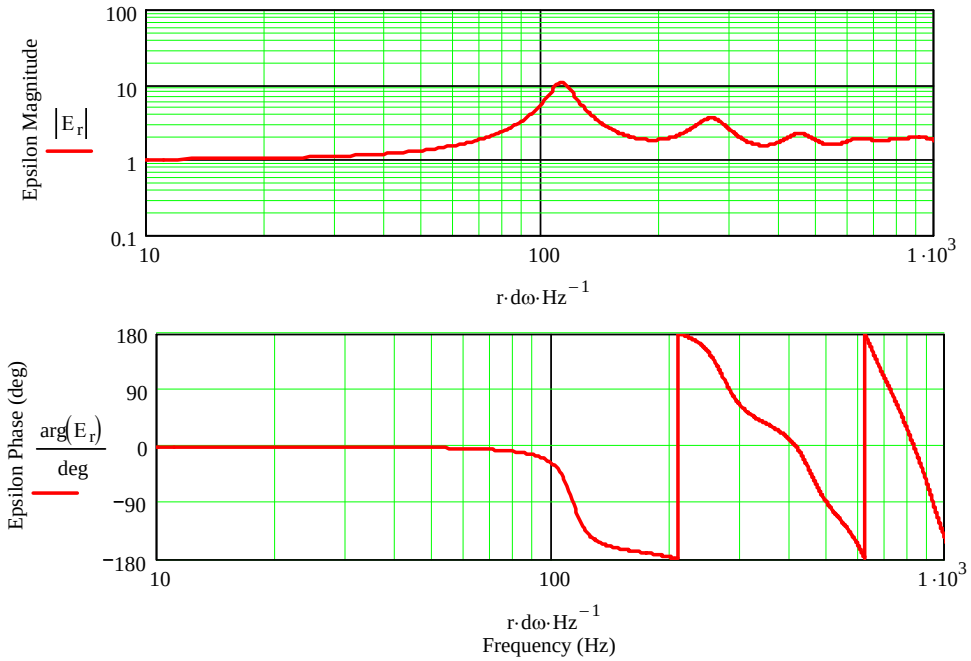

Figure 5.12 : Acoustic Impedance and Volume Velocity Ratio for S_L / S_0 = 5 in Table 5.2

Acoustic Impedance at the Throat of the Horn

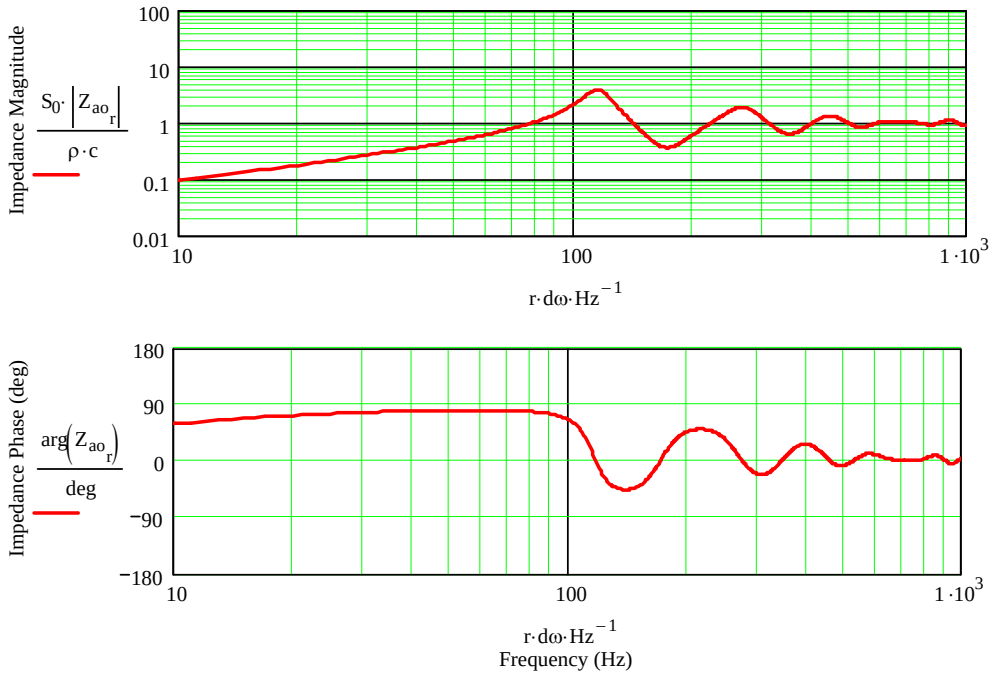

E = (Volume Velocity at the Mouth of the Horn) / (Volume Velocity at the Throat of the Horn)

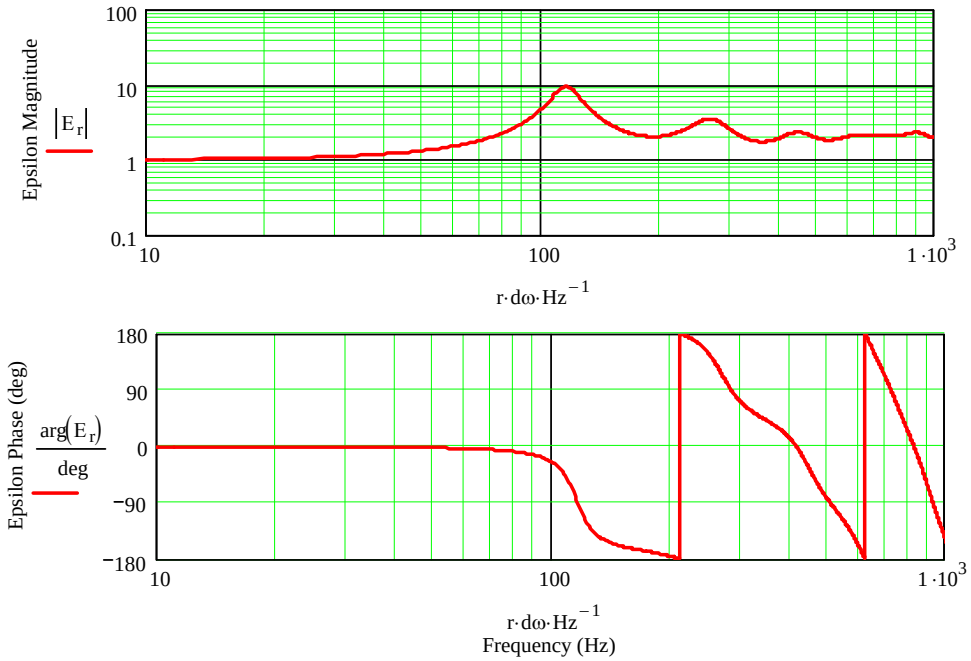

Figure 5.13 : Acoustic Impedance and Volume Velocity Ratio for S_L / S_0 = 10 in Table 5.2

Acoustic Impedance at the Throat of the Horn

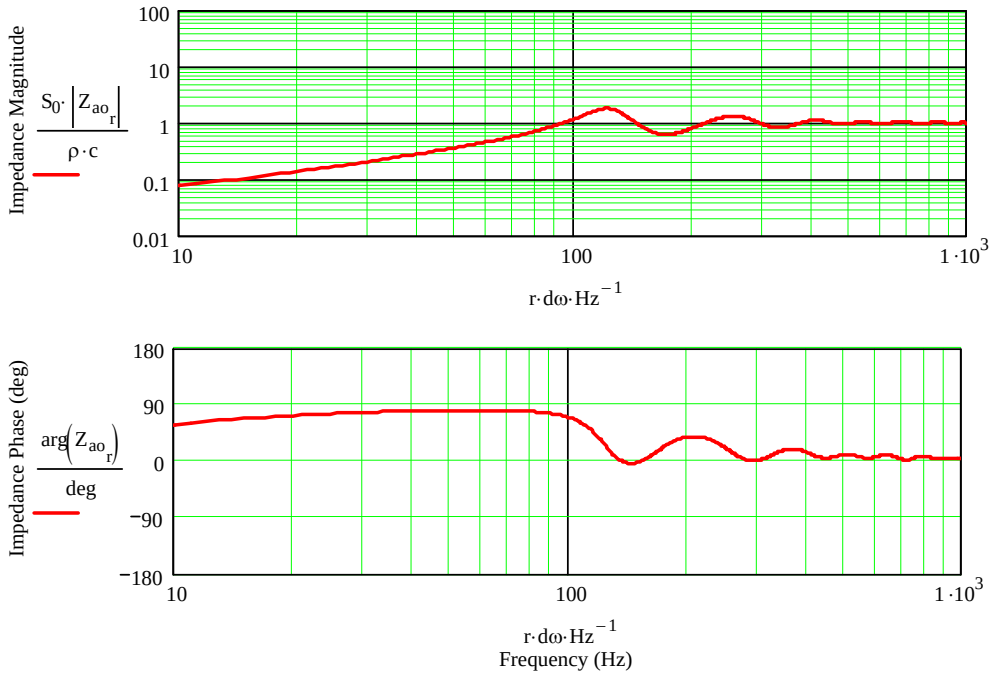

E = (Volume Velocity at the Mouth of the Horn) / (Volume Velocity at the Throat of the Horn)

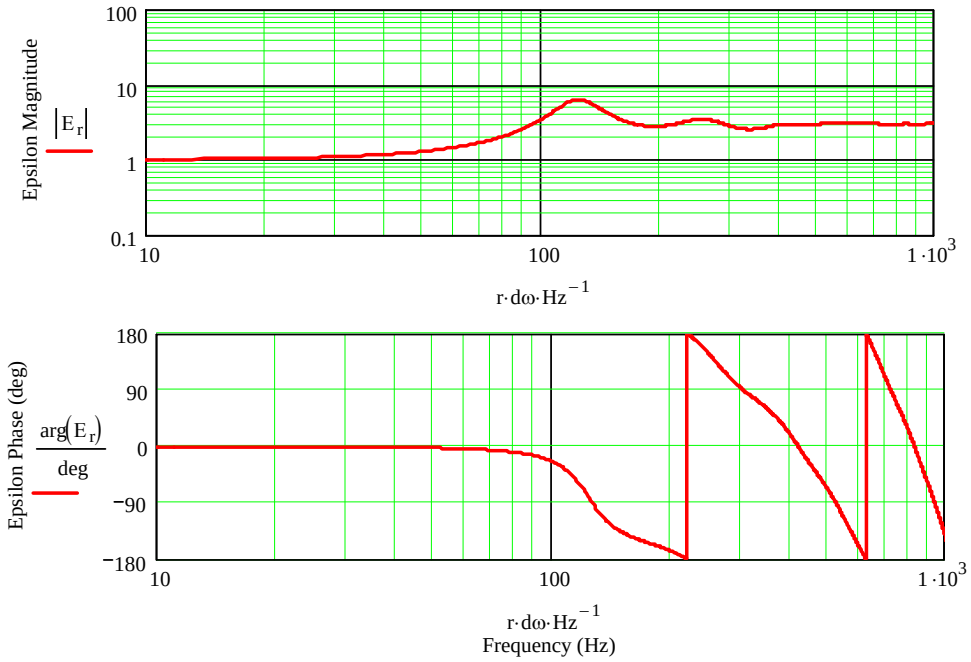

Figure 5.14 : Acoustic Impedance and Volume Velocity Ratio for S_L / S_0 = 15 in Table 5.2

Acoustic Impedance at the Throat of the Horn

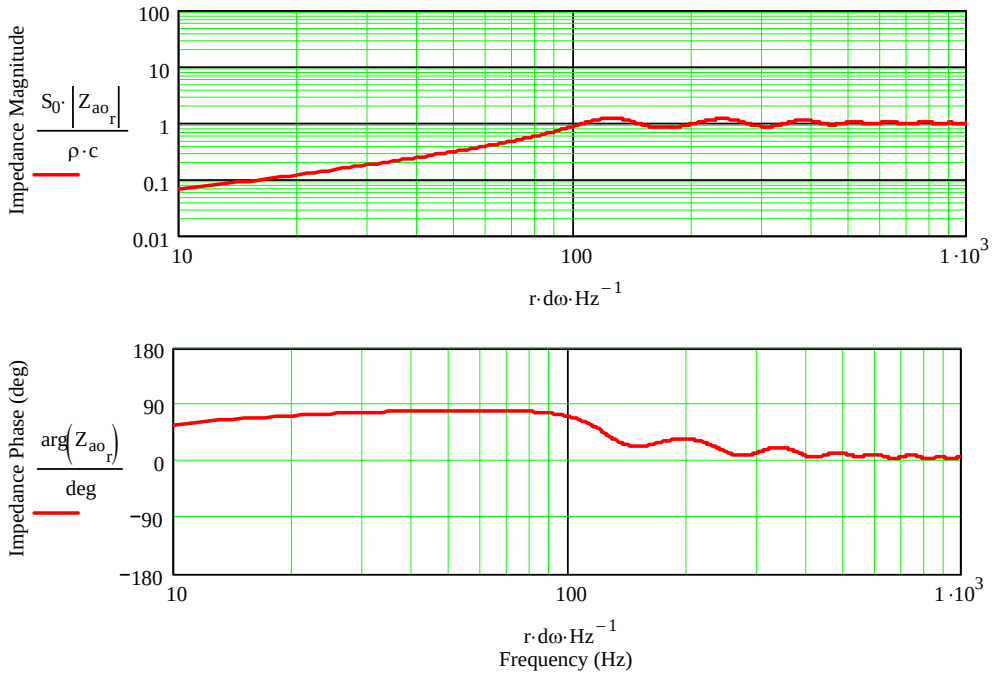

E = (Volume Velocity at the Mouth of the Horn) / (Volume Velocity at the Throat of the Horn)

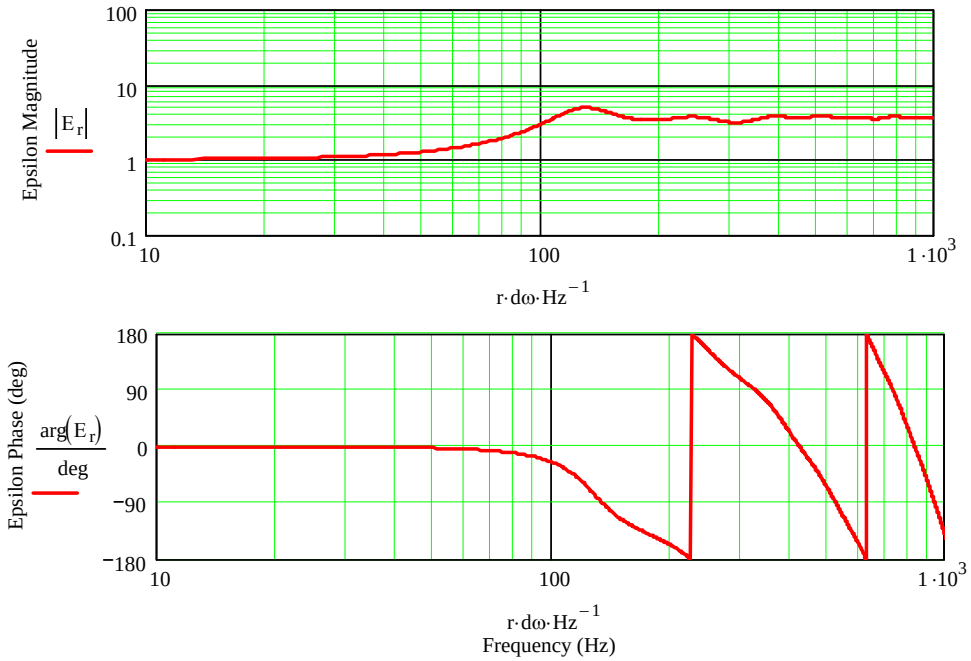

Figure 5.15 : Acoustic Impedance and Volume Velocity Ratio for S_L / S_0 = 20 in Table 5.2

Acoustic Impedance at the Throat of the Horn

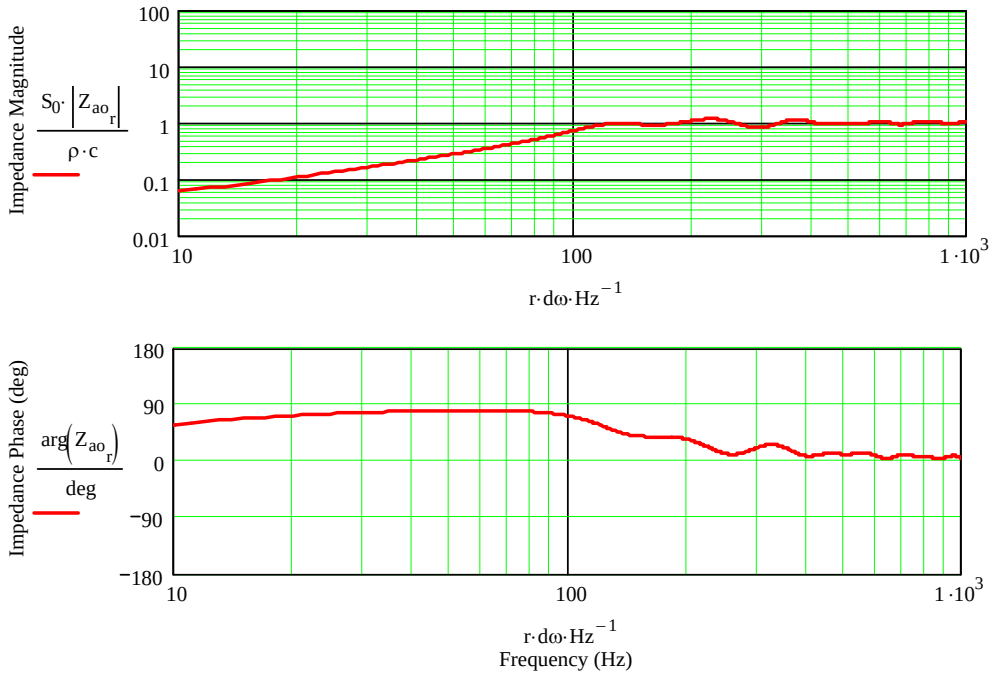

E = (Volume Velocity at the Mouth of the Horn) / (Volume Velocity at the Throat of the Horn)

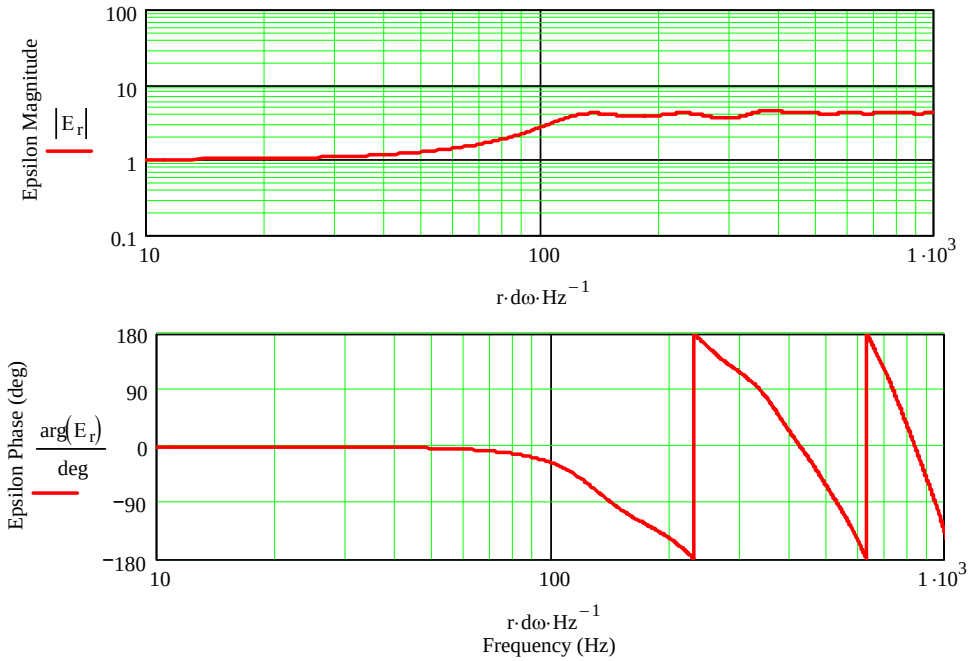

Figure 5.16 : Circular Horn Mouth Acoustic Impedance

Red Curve - Real Part
Blue Curve - Imaginary Part

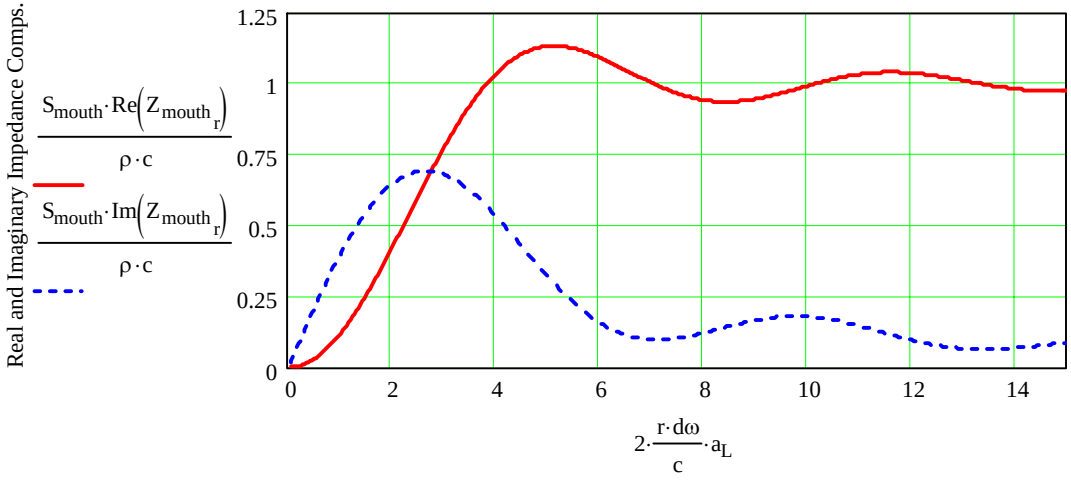

Linear and Conical Horn Geometries :

All of the preceding equations and plots have only addressed exponential horn geometries. Equations (5.1) and (5.2) were both derived based on the closed form solution of the 1D wave equation for an exponential horn. However, Equation (5.3) is derived based on a circular piston vibrating in an infinite baffle and is applicable to any horn flare geometry. In Section 3.0, it was shown that Equation (5.3) could also be applied to a square piston vibrating in an infinite baffle without any real loss of accuracy. To gain some insight into the behavior of other horn geometries, sized using Equations (5.1), (5.2), and (5.3), two additional cases are analyzed and presented.

Table 5.3 presents the horn geometries analyzed. In the original MathCad front and back loaded worksheets, three horn options were available including an exponential geometry and additionally linear and conical horn geometries. Figures 5.17, 5.18, and 5.19 show the acoustic impedance and the ratio of volume velocities for each of these horn geometries.

Table 5.3 : Two Additional Horn Geometries Based on Horn C in Table 5.1

Horn	S_0	S_L / S_0	S_L	L	Geometry	Figure
i	0.047	20	0.942	0.820	Exponential	5.17
j	0.047	20	0.942	0.820	Linear	5.18
k	0.047	20	0.942	0.820	Conical	5.19
Units	m^2	---	m^2	m	---	---

After reviewing Figures 5.18 and 5.19, it should be obvious that the alternate horn geometries perform differently compared to the exponential horn geometry. The conical geometry does not reach constant values of acoustic impedance and volume velocity ratio until much higher in the frequency range. The linear geometry exhibits a rounded peak at the 100 Hz cut-off frequency followed by a significant sag in the acoustic impedance over a wide frequency range.

Figure 5.17 : Acoustic Impedance and Volume Velocity Ratio for the Exponential Horn Geometry in Table 5.3

Acoustic Impedance at the Throat of the Horn

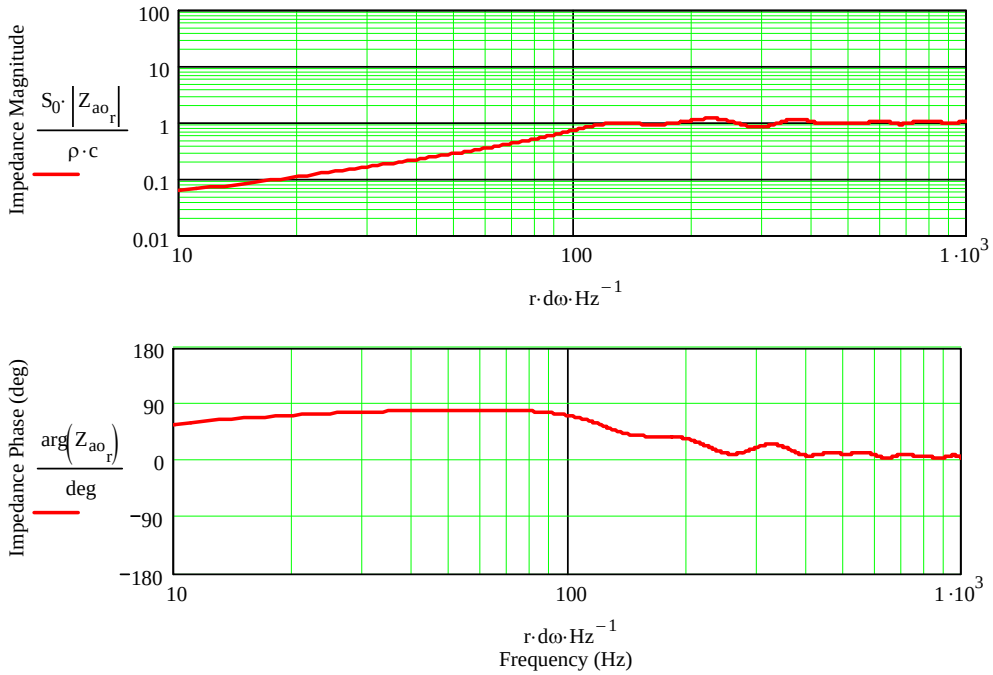

E = (Volume Velocity at the Mouth of the Horn) / (Volume Velocity at the Throat of the Horn)

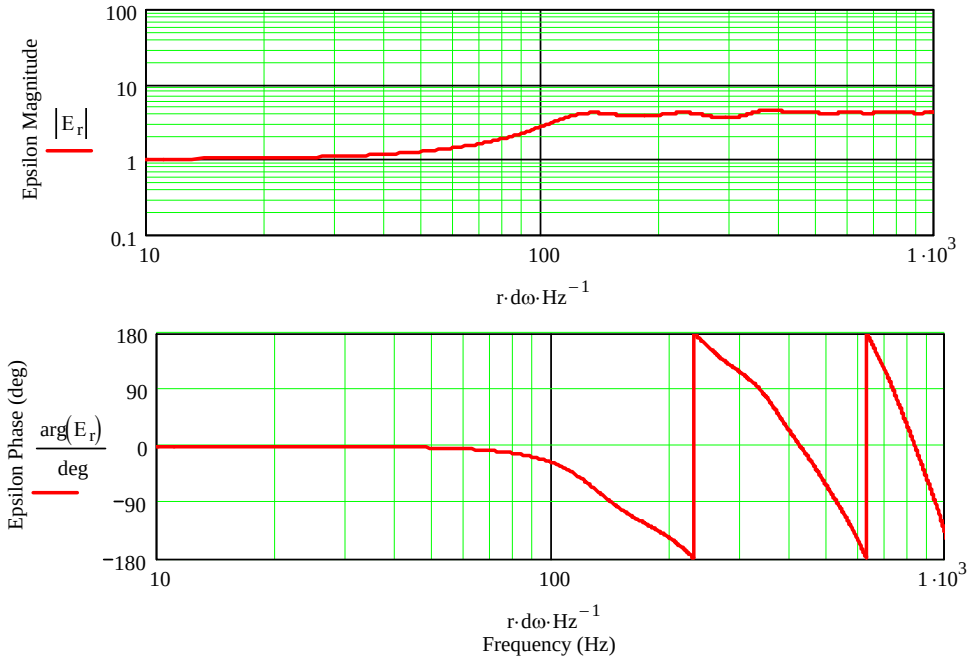

Figure 5.18 : Acoustic Impedance and Volume Velocity Ratio for the Linear Horn Geometry in Table 5.3

Acoustic Impedance at the Throat of the Horn

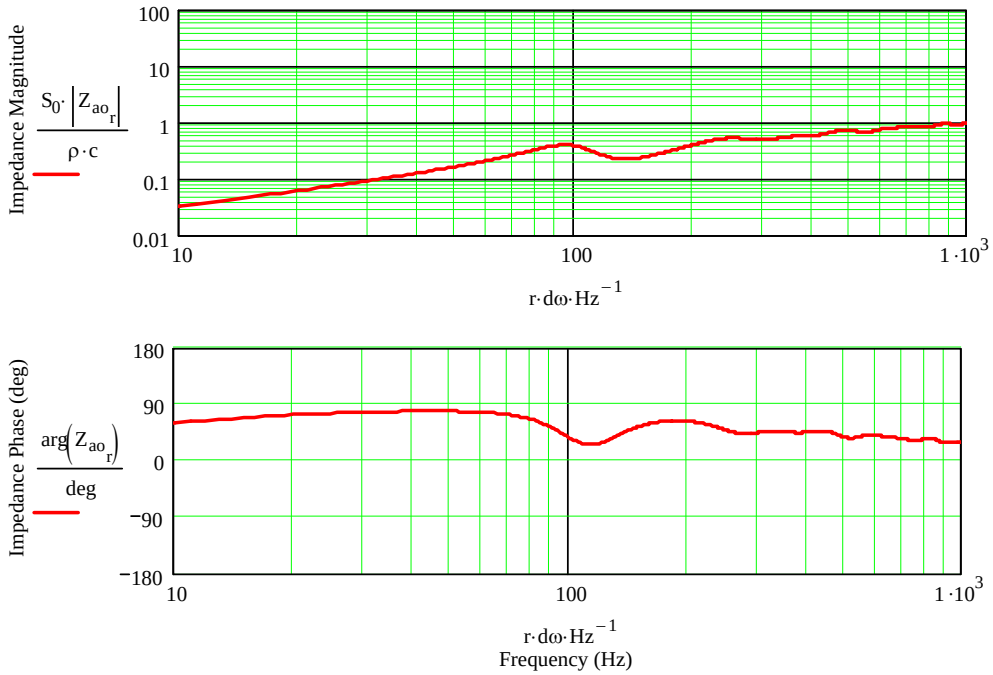

E = (Volume Velocity at the Mouth of the Horn) / (Volume Velocity at the Throat of the Horn)

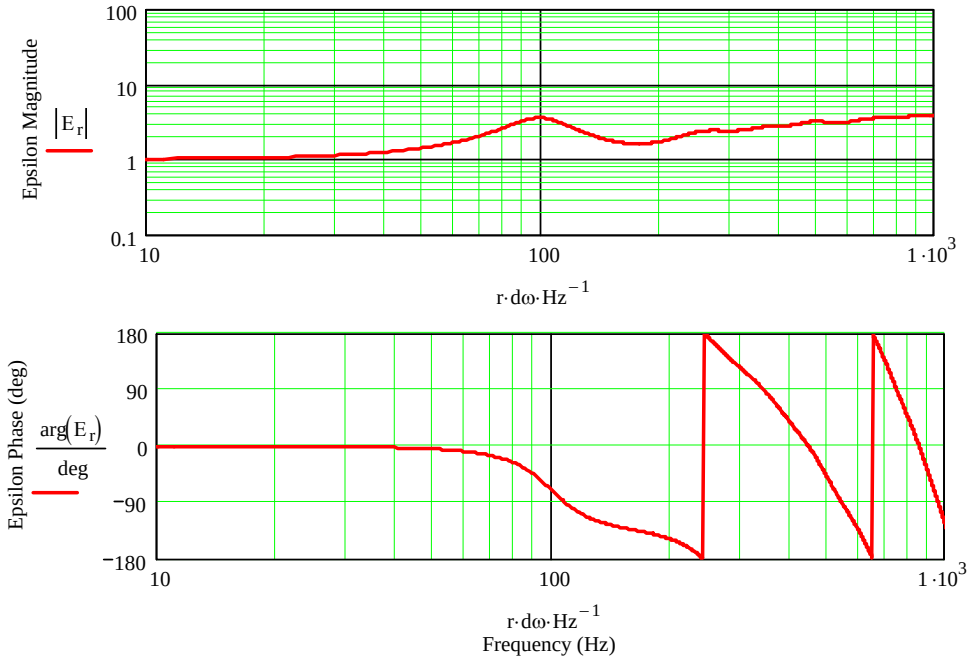

Figure 5.19 : Acoustic Impedance and Volume Velocity Ratio for the Conical Horn Geometry in Table 5.3

Acoustic Impedance at the Throat of the Horn

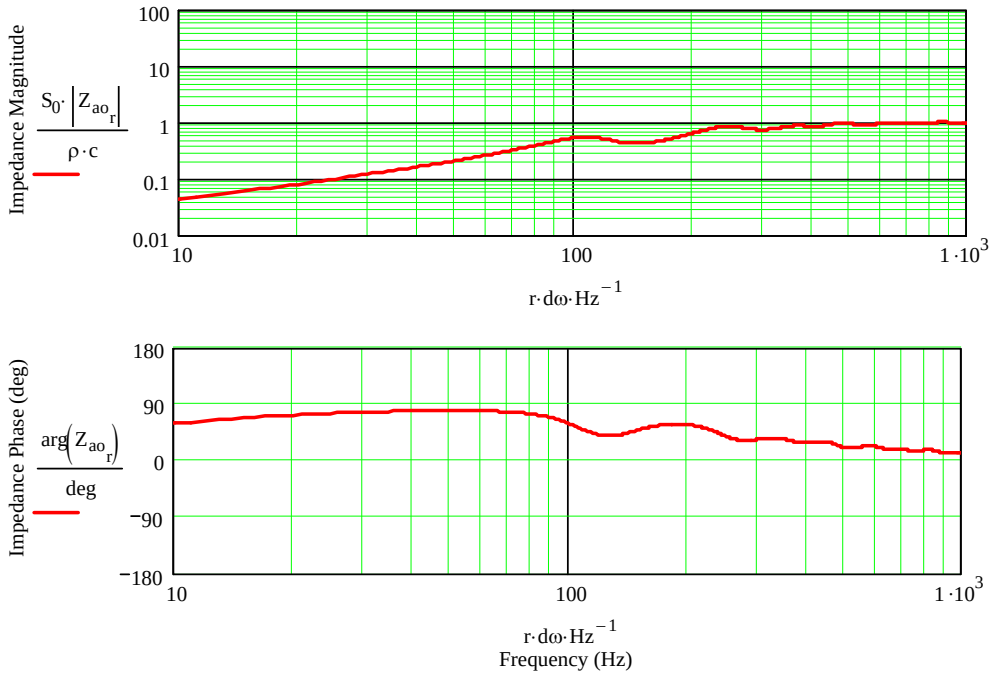

E = (Volume Velocity at the Mouth of the Horn) / (Volume Velocity at the Throat of the Horn)

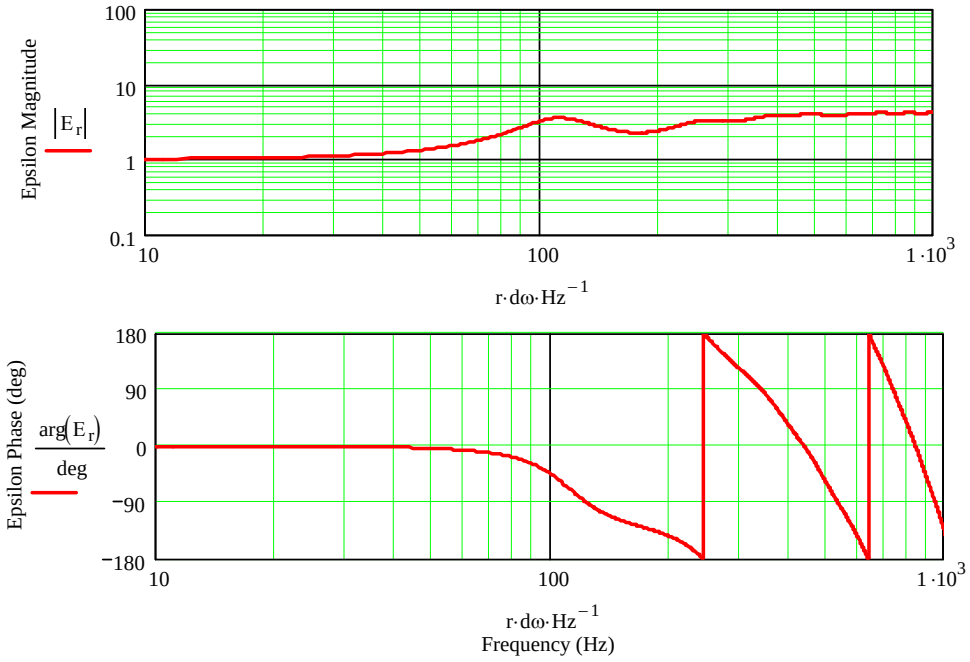

Summary :

The physics that make a horn work have been explored. Simple equations to size the geometry for a consistent exponential horn were derived. Exponential horn behavior was examined for various sized consistent horns all having the same lower cut-off frequency. It was also demonstrated that the application of these sizing equations to alternate horn geometries leads to different acoustic impedance and volume velocity ratio curve profiles.

An equation was derived for calculating the appropriate coupling chamber volume, between the driver and the throat of a horn, which will produce a predictable higher cut off frequency. This equation is applicable to any horn geometry operating well above the horn's lower cut-off frequency.

Armed with the equations derived in this section, the study of front and back loaded horn speaker systems is now possible. The following sections will examine the design of front and back loaded horns for a generic driver using the Thiele / Small parameters.